

# First-order corrections to semiclassical Gaussian partition functions for clusters of atoms

Holger Cartarius, Eli Pollak

Chemical Physics Department, Weizmann Institute of Science, 76100 Rehovot, Israel

## Abstract

Gaussian approximations to the Boltzmann operator have proven themselves in recent years as useful tools for the study of the thermodynamic properties of rare gas clusters. They are, however, not necessarily correct at very low temperatures. In this article we introduce a first-order correction term to the frozen Gaussian imaginary time propagator and apply it to the argon trimer. Our findings show that the correction term provides objective access to the quality of the propagator's results and clearly defines the "best" Gaussian width parameter. The strength of the correction monitored as a function of the temperature indicates that the results of the Gaussian propagator become questionable below a certain temperature. The interesting thermodynamic transition from a bounded trimer to three body dissociation lies in the temperature range for which the Gaussian approximation is predicted to be accurate.

*Keywords:* clusters, quantum thermodynamics, Gaussian approximations, first-order corrections, argon trimer

*PACS:* 36.40.-c, 03.65.Sq, 05.30.-d

## 1. Introduction

The imaginary time or Boltzmann operator  $\exp(-\beta\hat{H})$  belongs to the most important quantities needed for understanding the equilibrium properties of multi-dimensional systems at finite temperatures. The derivatives of its trace give access to the mean energy and specific heat, which allow for the investigation of thermodynamic properties of atomic clusters [1–7]. For systems with many degrees of freedom it is, however, still a challenge to evaluate the Boltzmann operator although it is accessible with Monte Carlo methods [8–10], since the necessary integrals can become numerically expensive, in particular at low temperatures. Approximations are essential to evaluate the Boltzmann operator for clusters of a few dozen atoms.

Semiclassical initial value representations propagating Gaussian wave packets of the form

$$\langle \mathbf{x} | g \rangle = \left( \pi^{3N} |\det \mathbf{G}(\tau)| \right)^{-1/4} \times \exp \left( -\frac{1}{2} [\mathbf{x} - \mathbf{q}(\tau)]^T \mathbf{G}(\tau)^{-1} [\mathbf{x} - \mathbf{q}(\tau)] + \gamma(\tau) \right), \quad (1)$$

for the Boltzmann operator have been developed [3, 11, 12] and successfully applied to the study of thermodynamic properties of clusters [3, 4, 6, 11, 13, 14]. In particular the time-evolved Gaussian approximation developed by Mandelshtam and co-workers [3, 11] has become an important tool which has been applied to thermodynamic properties of a large number of clusters [3, 4, 6, 11, 13]. This method is based on so-called *thawed* Gaussian wave packets, where the matrix of Gaussian

width parameters  $\mathbf{G}(\tau)$  changes with (imaginary) time  $\tau$ . Recently a *frozen* Gaussian propagator with a constant width matrix  $\mathbf{G}(\tau) = \mathbf{G}(0)$  suggested by Zhang et al. [12] was shown to provide results competitive with the time-evolved Gaussian approximation using a single particle ansatz [14] to simplify the computation of the time-dependent width matrix. Since no equations of motion for the  $N \times N$  elements of  $\mathbf{G}$  have to be propagated, the frozen Gaussian method is numerically much cheaper.

Despite the large success and broad applicability of Gaussian methods for the evaluation of the mean energy and the specific heat of clusters one has to keep in mind that they are semiclassical approximations. As pointed out by Liu and Miller [15] they are not expected to be accurate at very low temperatures where quantum effects are large. In the simplest case one observes a shift of the ground state energy away from the exact result [14]. The low-temperature range is, however, very often the most important and crucial for the thermodynamic properties of rare gas cluster. For example, Gaussian based computations on clusters of light atoms, e.g.,  $\text{Ne}_{13}$  and  $\text{Ne}_{38}$  [4, 6], predict novel low temperature quantum effects such as liquid-like zero temperature structures of  $\text{Ne}_{38}$  as compared to a solid-like structure predicted from classical mechanics [16]. These predictions are based on the Gaussian approximation [3, 6, 11, 13, 15] and have to be verified.

A systematic approach connecting the Gaussian semiclassical initial value approximations with exact quantum mechanics is the generalized time-dependent perturbation approach developed by Pollak and coworkers [12, 17]. Within this framework the Gaussian approximations can be considered as a lowest-order approximation of a series converging to the exact quantum Boltzmann operator. It has been shown that both the thawed and frozen Gaussian versions of this series converge rapidly to

*Email address:* Holger.Cartarius@weizmann.ac.il (Holger Cartarius)

the numerically exact answer for a one-dimensional double well potential [12, 18]. In this paper we demonstrate that the corrections to the Gaussian imaginary time propagator are also practically applicable to higher-dimensional systems, in particular to atomic clusters. To do so, we apply the frozen Gaussian series to the partition function of the argon trimer and calculate its first-order correction. We show that the correction helps to estimate the quality of the results and provides objective access to the validity of the Gaussian approximations. With the first-order terms it is possible to identify a border temperature below which the Gaussian results become questionable. This result clearly states that the dissociation process [7] discussed earlier with Gaussian approximations [14] is correctly described by the frozen Gaussian imaginary time propagator since it appears in the allowed temperature range.

The Gaussian width of the frozen Gaussian propagator is a free parameter but has an important impact on the accuracy of the physical quantities calculated with the approximation. It is demonstrated in this article that the first-order correction provides an unambiguous method for optimizing the value which is based on minimizing the ratio between the first-order correction to the zeroth-order term for the Boltzmann operator. This choice improves the results for the mean energy and the specific heat. Including the first-order correction they reach the same quality as a fully-coupled thawed Gaussian computation over a wide range of temperatures.

This article is organized as follows. In Sec. 2 we review the most important parts of the frozen Gaussian series representation of the Boltzmann operator and introduce the first-order correction to the partition function for clusters of atoms. The theory is then applied to the argon trimer in Sec. 3. We introduce the system (Sec. 3.1), show how the first-order correction term may be used to determine the best width parameter (Sec. 3.2), consider the influence of an artificial confinement on the correction (Sec. 3.3) and present the first-order corrected mean energy and specific heat for the dissociation process of the cluster (Sec. 3.4), which allow for a clear statement on the quality of the Gaussian approximation. The required numerical effort is analyzed in Sec. 4. Conclusions are drawn in Sec. 5.

## 2. Frozen Gaussian approximation to the partition function and first-order corrections

### 2.1. Frozen Gaussian series representation

Zhang et al. [12] proposed a frozen Gaussian form of the imaginary time propagator  $K(\beta) = \exp(-\beta\hat{H})$  at inverse temperature  $\beta = 1/(kT)$  and developed its higher-order corrections in the framework of the generalized time-dependent perturbation series [17, 19, 20]. The frozen Gaussian coherent state has the form

$$\langle \mathbf{x} | g(\mathbf{p}(\tau), \mathbf{q}(\tau), \mathbf{\Gamma}) \rangle = \left( \frac{\det(\mathbf{\Gamma})}{\pi^{3N}} \right)^{1/4} \times \exp\left( -\frac{1}{2} [\mathbf{x} - \mathbf{q}(\tau)]^T \mathbf{\Gamma} [\mathbf{x} - \mathbf{q}(\tau)] + \frac{i}{\hbar} \mathbf{p}^T(\tau) \cdot [\mathbf{x} - \mathbf{q}(\tau)] \right), \quad (2)$$

with the symmetric positive definite matrix of constant width parameters  $\mathbf{\Gamma}$  and the dynamical variables  $\mathbf{q}(\tau)$  and  $\mathbf{p}(\tau)$ . Approximating a solution to the Bloch equation

$$-\frac{\partial}{\partial \tau} |q_0, \tau\rangle = H |q_0, \tau\rangle \quad (3)$$

by propagating a frozen Gaussian wave packet, one finds that the imaginary time propagator matrix element has the form

$$\begin{aligned} \langle \mathbf{x}' | K_0(\tau) | \mathbf{x} \rangle &= \det(\mathbf{\Gamma}) \exp\left( -\frac{\hbar^2}{4} \text{Tr}(\mathbf{\Gamma}\tau) \right) \\ &\times \sqrt{\det\left( 2[\mathbf{1} - \exp(-\hbar^2\mathbf{\Gamma}\tau)]^{-1} \right)} \\ &\times \exp\left( -\frac{1}{4} [\mathbf{x}' - \mathbf{x}]^T \mathbf{\Gamma} [\tanh(\hbar^2\mathbf{\Gamma}\tau/2)]^{-1} [\mathbf{x}' - \mathbf{x}] \right) \\ &\times \int \frac{d\mathbf{q}^{3N}}{(2\pi)^{3N}} \exp\left( -2 \int_0^{\tau/2} d\tau' \langle V(\mathbf{q}(\tau')) \rangle \right. \\ &\left. - [\bar{\mathbf{x}} - \mathbf{q}(\tau/2)]^T \mathbf{\Gamma} [\bar{\mathbf{x}} - \mathbf{q}(\tau/2)] \right) \quad (4) \end{aligned}$$

with  $\bar{\mathbf{x}} = (\mathbf{x}' + \mathbf{x})/2$ . The only remaining dynamical variables in this representation of the propagator are the components of the vector  $\mathbf{q}(\tau)$ , which follow the equations of motion

$$\frac{\partial \mathbf{q}(\tau)}{\partial \tau} = -\mathbf{\Gamma}^{-1} \langle \nabla V(\mathbf{q}(\tau)) \rangle. \quad (5)$$

The angle brackets symbolize Gaussian averaged quantities of the form

$$\begin{aligned} \langle h(\mathbf{q}) \rangle &= \left( \frac{\det(\mathbf{\Gamma})}{\pi^{3N}} \right)^{1/2} \\ &\times \int_{-\infty}^{\infty} d\mathbf{x}^{3N} \exp(-[\mathbf{x} - \mathbf{q}]^T \mathbf{\Gamma} [\mathbf{x} - \mathbf{q}]) h(\mathbf{x}). \quad (6) \end{aligned}$$

In the framework of the generalized time-dependent perturbation theory,  $K_0(\tau)$  is the zeroth-order approximation to the exact Boltzmann operator. Since the Bloch equation (3) is not solved exactly by the propagator (4), one can define the correction operator [17]

$$C(\tau) = -\frac{\partial}{\partial \tau} K_0(\tau) - H K_0(\tau). \quad (7)$$

The formal solution of Eq. (7) is

$$K_0(\tau) = K(\tau) - \int_0^\tau d\tau' K(\tau - \tau') C(\tau'). \quad (8)$$

With the assumption that the exact propagator  $K(\tau)$  can be expressed in terms of a series

$$K(\tau) = \sum_{n=0}^{\infty} K_j(\tau), \quad (9)$$

where  $K_j(\tau) \sim C(\tau)^j$  are terms with ascending power in the small correction, one can write down the recursion relation

$$K_{j+1}(\tau) = \int_0^\tau d\tau' K_j(\tau - \tau') C(\tau') \quad (10)$$

for the calculation of higher-order terms.

## 2.2. First-order corrections to the partition function

In the framework of the series expansion the lowest-order approximation to the quantum partition function is simply the trace of the zeroth-order propagator [12],

$$Z_0(\beta) = \text{Tr}[K_0(\beta)] = \sqrt{\det(\mathbf{\Gamma})} \exp\left(-\frac{\hbar^2}{4} \text{Tr}(\mathbf{\Gamma})\beta\right) \\ \times \sqrt{\det([\mathbf{1} - \exp(-\hbar^2\mathbf{\Gamma}\beta)]^{-1})} \\ \times \int_{-\infty}^{\infty} \frac{d\mathbf{q}^{3N}}{(2\pi)^{N/2}} \exp\left(-2 \int_0^{\beta/2} d\tau \langle V(\mathbf{q}(\tau)) \rangle\right). \quad (11)$$

Its first-order corrected counterpart

$$Z_1(\beta) = Z_0(\beta) + Z_{C1}(\beta) \quad (12a)$$

is obtained in a similar way. The first-order correction to the propagator is evaluated according to Eq. (10) and then the correction term for the partition function is

$$Z_{C1}(\beta) = \text{Tr}[K_1(\beta)] \\ = \int_0^{\beta} d\tau \int d\mathbf{x}^{3N} \int d\mathbf{x}'^{3N} \langle \mathbf{x}' | K_0(\beta - \tau) | \mathbf{x} \rangle \langle \mathbf{x} | C(\tau) | \mathbf{x}' \rangle. \quad (12b)$$

More details of the correction operator and the first-order term to the partition function can be found in Appendix A. In particular it is shown, how the  $\mathbf{x}'$  and  $\mathbf{x}$  integrations in Eq. (12b) can be performed analytically if the potential of the system can be expressed in terms of Gaussians. This makes the evaluation of the correction terms efficient.

Note that the first-order correction term (12b) is not symmetric. Here we used the “left” correction operator defined by Zhang et al. [12]. This has, however, no influence on the partition function due to the trace in Eq. (12b).

## 3. First-order calculations for the argon trimer

### 3.1. Potential and confinement

To be consistent with previous studies of the system [7, 14, 21] we model the pairwise interaction of the argon atoms by a Morse potential

$$V(r_{ij}) = D \left( \exp[-2\alpha(r_{ij} - R_e)] - 2 \exp[-\alpha(r_{ij} - R_e)] \right) \quad (13)$$

with the distance  $r_{ij}$  between particles  $i$  and  $j$  and the Morse parameters  $D = 99.00 \text{ cm}^{-1}$ ,  $\alpha = 1.717 \text{ \AA}^{-1}$ , and  $R_e = 3.757 \text{ \AA}$ . Since the Gaussian averaged quantities according to Eq. (6) and the  $\mathbf{x}'$  and  $\mathbf{x}$  integrations in the first-order correction term (12b) can be performed analytically if the potential can be expressed in terms of Gaussians, we fitted the Morse potential (13) to a sum of three Gaussians

$$V(|\mathbf{r}_i - \mathbf{r}_j|) = \sum_{p=1}^3 c_p e^{-\alpha_p r_{ij}^2}, \quad r_{ij} = |\mathbf{r}_i - \mathbf{r}_j|, \quad (14)$$

with the parameters listed in Table 1.

Table 1: Parameters used in the Gaussian representation (14) of the potential, taken from Ref. [14].

$p$	$c_p [\text{cm}^{-1}]$	$\alpha_p [\text{\AA}^{-2}]$
1	$3.296 \times 10^5$	0.6551
2	$-1.279 \times 10^3$	0.1616
3	$-9.946 \times 10^3$	6.0600

Since all  $\mathbf{x}'$  and  $\mathbf{x}$  integrations in the zeroth-order approximation and the first-order correction term of the propagator can be performed analytically with the Gaussian potential (14) only the integration in the  $\mathbf{q}$  space and the imaginary time integration in Eq. (12b) remain for numerical computation. The  $\tau$  integration is one-dimensional and can be done with a standard integrator. The multi-dimensional Monte Carlo sampling in the  $\mathbf{q}$  variables is done with a standard Metropolis algorithm as outlined in Ref. [3].

To converge the integrals the  $\mathbf{q}$  space is restricted by the condition  $|\mathbf{q} - \mathbf{R}_{\text{cm}}| < R_c$ , where  $R_c$  is a confining radius and  $\mathbf{R}_{\text{cm}}$  is the center of mass of the cluster. That is, no atom may leave the center of mass beyond a certain distance  $R_c$ . It is also possible to introduce the confinement via an additional steep potential [2] as

$$V_c(\mathbf{r}) \propto \sum_{i=1}^N \left( \frac{r_i - \mathbf{R}_{\text{cm}}}{R_c} \right)^{20}. \quad (15)$$

As has been shown previously [2, 14, 22], the value of  $R_c$  has a critical influence on the thermodynamic properties. For the first-order correction term (12b) two  $\mathbf{q}$  integrations, viz. in the propagator and in the correction operator, have to be taken into account. Here, the restriction on  $\mathbf{q}$  is applied for the propagator part (4). Due to the coupling via  $\mathbf{x}'$  and  $\mathbf{x}$  the restriction automatically affects also the  $\mathbf{q}$  variable in the correction operator. More details can be found in Appendix A.

In this article we concentrate on a confinement of  $R_c = 10 \text{ \AA}$ . It is known that this confinement does not describe the dissociation process fully since it is too restrictive. However, the restricted cluster shows a very broad transition from the bounded system to three free particles, and thus allows for a clear analysis of the correction term’s influence on the results around the dissociation, which is the interesting physical effect.

### 3.2. Choice of the width parameter

In the frozen Gaussian ansatz the matrix of width parameters  $\mathbf{\Gamma}$  is constant in imaginary time  $\tau$ , however, the choice of  $\mathbf{\Gamma}$  has a critical influence on the quality of the results [12]. In a previous study [14] we found that the width matrix

$$\mathbf{\Gamma} = \begin{pmatrix} (\mathbf{D}_1 + 2\mathbf{D}_2)/3 & (\mathbf{D}_1 - \mathbf{D}_2)/3 & (\mathbf{D}_1 - \mathbf{D}_2)/3 \\ (\mathbf{D}_1 - \mathbf{D}_2)/3 & (\mathbf{D}_1 + 2\mathbf{D}_2)/3 & (\mathbf{D}_1 - \mathbf{D}_2)/3 \\ (\mathbf{D}_1 - \mathbf{D}_2)/3 & (\mathbf{D}_1 - \mathbf{D}_2)/3 & (\mathbf{D}_1 + 2\mathbf{D}_2)/3 \end{pmatrix} \quad (16)$$

with two  $3 \times 3$ -submatrices  $\mathbf{D}_1 = D_1 \mathbf{1}$  and  $\mathbf{D}_2 = D_2 \mathbf{1}$ , where  $\mathbf{1}$  is the  $3 \times 3$  identity matrix, provides results competitive with thawed Gaussian calculations using a single-particle ansatz. The

parameter  $D_1$  represents the free center of mass motion and should be chosen as small as possible. The Gaussian width for the relative coordinates is represented by  $D_2$ . In Ref. [14] an optimum value of  $D_2 = 25 \text{ \AA}^{-2}$  was found. It yielded the best approximation to a numerically exact path integral Monte Carlo calculation [7] and thawed Gaussian approximations [14]. In the same work it was found that all choices of  $D_1$  below a certain value lead to the same mean energies and that  $D_1 = 0.1 \text{ \AA}^{-2}$  belongs to this range in which  $D_1$  is small enough. These parameters also provide the best and lowest approximation to the ground state energy. Thus, the minimum of the ground state energy could also be used to search for the optimum value of the width parameters. It provides, however, no access to the quality of the results if the exact ground state energy is unknown.

A systematic, objective and internally consistent approach to the determination of the optimum width parameter is made possible by considering the first-order correction. The definition of the correction operator in Eq. (7) makes clear that it measures the deviation of the zeroth-order term from the exact result. One should thus minimize the ratio of the first-order [Eq. (12b)] and zeroth-order [Eq. (11)] contributions to the partition function by varying the width parameter matrix and thus find the optimum value.

In Fig. 1(a) we plot the ratio  $Z_{C1}/Z_0$  for several values of the parameters  $D_2$  and  $D_1 = 0.1 \text{ \AA}^{-2}$ . The data was calculated for a cluster with a confinement of  $R_c = 10 \text{ \AA}$ . The zeroth- and first-order mean energies in Fig. 1(b) visualize the transition from a bounded to an unbounded cluster. For temperatures at which the system is bounded, i.e.,  $T \lesssim 30 \text{ K}$  an optimum range for the width parameter at which the contribution of the correction term  $Z_{C1}$  is minimal can be found. Below the transition temperature the lines for  $D_2$  between  $20 \text{ \AA}^{-2}$  and  $30 \text{ \AA}^{-2}$  are close to each other, the smallest value is found for  $D_2 = 25 \text{ \AA}^{-2}$ . This confirms our previous zeroth-order study of the argon trimer [14], where the same value of  $D_2 = 25 \text{ \AA}^{-2}$  provided the best agreement with numerically exact path integral Monte Carlo methods. At higher temperatures, where the cluster passes through a transition to three almost free atoms, the situation changes. The ratio becomes smaller as the magnitude of  $D_2$  decreases. In the limit of three free particles, the frozen Gaussian approximation is exact, in the limit that the width matrix vanishes. One thus expects that in this limit, the smaller values of the width parameters would provide a better approximation.

### 3.3. Influence of the confining sphere

As already mentioned, for free particles, the frozen Gaussian propagator yields the exact partition function in the limit  $\Gamma \rightarrow \mathbf{0}$ . Thus, one expects that the free center of mass motion, described by  $D_1$ , demands  $D_1$  to be as small as possible. In practice one observes, however, that  $D_1$  shows a minimum correction at a finite value. This is a result of the confinement of the atoms, which has the same effect as adding a confining potential (15), i.e., the particles are not really free. The effect can be observed in Fig. 2, where the ratio  $Z_{C1}/Z_0$  is plotted for several choices of  $D_1$  and  $D_2 = 25 \text{ \AA}^{-2}$ . As can be seen the minimum

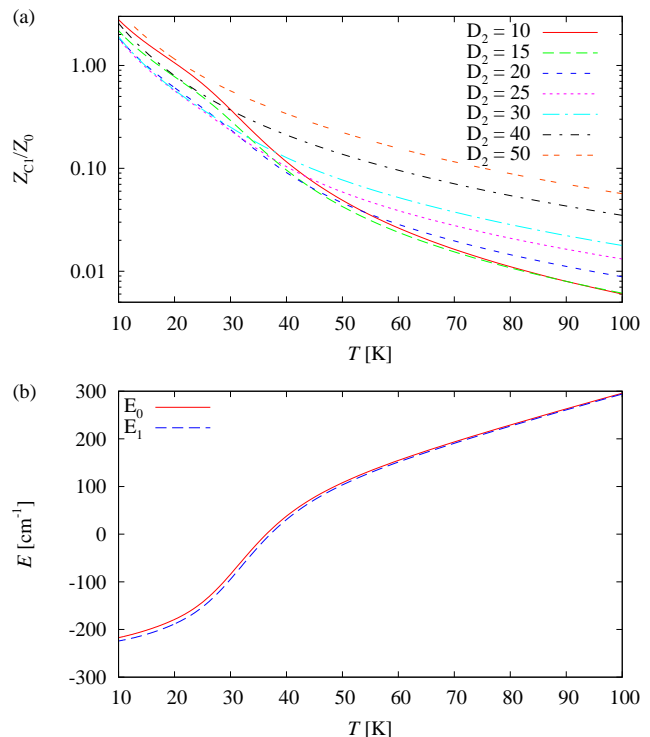


Figure 1: (a) The ratio of the contribution of the first- and zeroth-order terms in the series expansion of the partition function is plotted as a function of the temperature  $T$  for varying values of the width parameter  $D_2$  (given in units of  $\text{\AA}^{-2}$ ) and  $D_1 = 0.1 \text{ \AA}^{-2}$ . For the bounded system ( $T \lesssim 30 \text{ K}$ ) the range  $D_2 = 20 \dots 30 \text{ \AA}^{-2}$  leads to the minimal ratio whereas for temperatures above the transition temperature smaller values of  $D_2$  lead to smaller relative corrections. (b) The zeroth-order approximation to the mean energy  $E_0$  and its first-order corrected counterpart  $E_1$  is shown to visualize the transition from the bounded to the unbounded system for  $D_1 = 0.1 \text{ \AA}^{-2}$  and  $D_2 = 25 \text{ \AA}^{-2}$ .

correction is achieved for the finite values  $D_1 = 0.5 \dots 1 \text{ \AA}^{-2}$  if a confinement of  $R_c = 10 \text{ \AA}$  is used.

The influence of the confinement can also be found in the study of the width parameter  $D_2$  for the internal degrees of freedom. For high temperatures, i.e., in the limit of three free particles a smaller value of  $D_2$  should provide a better approximation. Thus, one expects always a smaller contribution  $Z_{C1}$  for smaller values of  $D_2$ . However, the strengths of the first-order corrections for  $D_2 = 10 \text{ \AA}^{-2}$  and  $D_2 = 15 \text{ \AA}^{-2}$  are almost the same in the high-temperature limit, even beyond the temperatures shown in the figure.

### 3.4. Correction at low temperatures and the first-order corrected mean energy

Figures 1(a) and 2 already indicate that the correction term increases in importance as the temperature is lowered. This is not surprising since an imaginary time propagation is performed approximately and the difference between the approximate and exact solutions is expected to increase with (imaginary) time. The behavior becomes even clearer in Fig. 3, where the relative strength of the first-order correction  $Z_{C1}/Z_0$  is plotted for the argon trimer with a confinement  $R_c = 10 \text{ \AA}$  and width

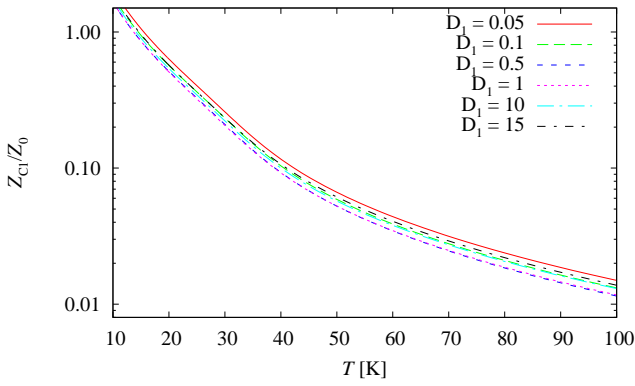


Figure 2: The ratio of the contribution of the first- and zeroth-order terms in the series expansion of the partition function is plotted as a function of the temperature  $T$  for varying values of the width parameter  $D_1$  (given in units of  $\text{\AA}^{-2}$ ) and  $D_2 = 25 \text{\AA}^{-2}$ . The minimal ratio is found in the range  $D_1 = 0.5 \dots 1 \text{\AA}^{-2}$ . The cluster is limited by a confinement with  $R_c = 10 \text{\AA}$ .

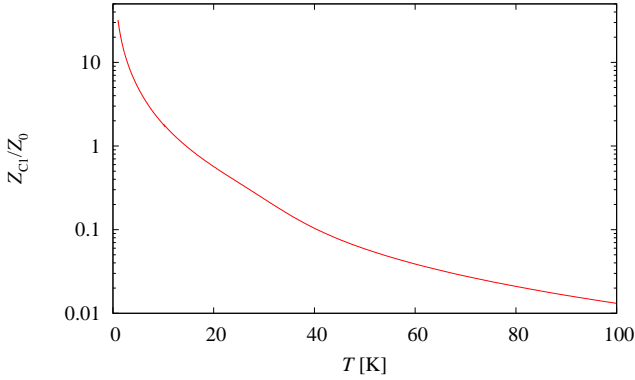


Figure 3: Relative strength of the first-order correction to the partition function at lower temperatures for  $R_c = 10 \text{\AA}$ ,  $D_1 = 0.1 \text{\AA}^{-2}$ , and  $D_2 = 25 \text{\AA}^{-2}$ . It diverges in the limit  $T \rightarrow 0$ .

parameters  $D_1 = 0.1 \text{\AA}^{-2}$ ,  $D_2 = 25 \text{\AA}^{-2}$  down to a temperature of  $T = 1 \text{ K}$ . It increases drastically and shows a diverging behavior in the limit  $T \rightarrow 0$ , i.e.,  $\beta \rightarrow \infty$ . The increasing importance of the first-order correction term at low temperatures is consistent with our previous zeroth-order study of the system, where we found that the accuracy of the frozen Gaussian approximation gets worse as  $T \rightarrow 0$  and the cluster approaches the ground state [14]. At low temperatures, quantum effects are strong and, in particular, the Gaussian (zeroth-order) approximations cannot reproduce the exact ground state energy  $E_{GS}$  of the cluster. The Gaussian form imposed on the wave function is too severe and the ground state energy obtained from the zeroth-order approximation is found to be slightly higher than the exact ground state energy ( $E_0 = E_{GS} + \Delta E$  and  $\Delta E > 0$ ).

To further understand the divergence of the first-order term, we may assume that for large  $\beta$  only the ground state contributes to the partition function and that the exact partition function  $Z$  and its zeroth-order approximated counterpart  $Z_0$  behave as

$$Z \approx e^{-\beta E_{GS}}, \quad Z_0 \approx e^{-\beta(E_{GS} + \Delta E)}. \quad (17)$$

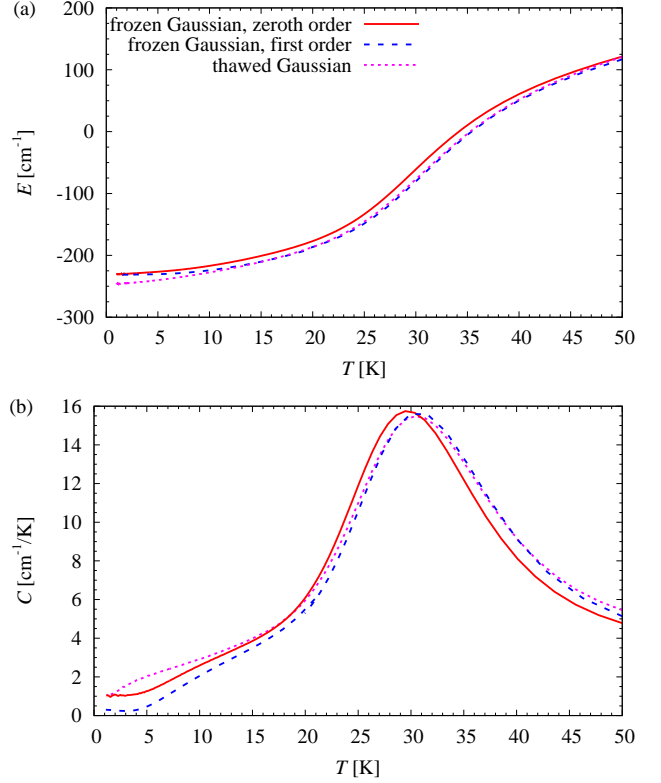


Figure 4: (a) Temperature dependence of the mean energy of the argon trimer for  $R_c = 10 \text{\AA}$ ,  $D_1 = 0.1 \text{\AA}^{-2}$ , and  $D_2 = 25 \text{\AA}^{-2}$ . Shown are the zeroth-order (solid line) and first-order (dashed line) frozen Gaussian results, and the fully-coupled thawed Gaussian approximation (dotted line). (b) Specific heat for the same parameters. Both calculations indicate a substantial improvement due to the first-order correction in the temperature region of the transition and above. For lower temperatures the correction breaks down, indicating that the frozen Gaussian approximation is no longer sufficiently accurate.

Thus, a first-order correction which is valid also for large  $\beta$  would be expected to diverge, since  $Z/Z_0 \approx e^{\beta \Delta E}$ .

More interesting is, however, the influence of the first-order correction on the derivatives of the partition function, which are required for the physically meaningful average energy

$$E = kT^2 \frac{\partial \ln Z}{\partial T} \quad (18a)$$

and specific heat

$$C = \frac{\partial E}{\partial T}. \quad (18b)$$

Figure 4 shows the temperature dependence of the mean energy and specific heat of the argon trimer for  $R_c = 10 \text{\AA}$ ,  $D_1 = 0.1 \text{\AA}^{-2}$ , and  $D_2 = 25 \text{\AA}^{-2}$ , i.e., the same parameters as in Fig. 3. The frozen Gaussian results for the zeroth- and first-order approximations are compared with a fully-coupled thawed Gaussian approximation which, as discussed elsewhere [14] is expected to be more accurate than the frozen Gaussian approximation. As one can see in Fig. 4(a) the first-order correction for the frozen Gaussian approximation brings the resulting estimate closer to the fully-coupled thawed Gaussian estimate over most of the temperature range studied. However, for temperatures  $T \lesssim 12 \text{ K}$  the first-order correction to the energy becomes

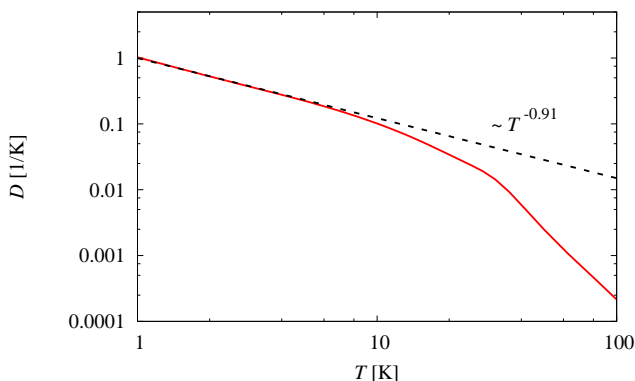


Figure 5: Double logarithmic plot of the difference  $D$  between the first derivatives of the logarithms of the zeroth- and first-order partition functions as defined in Eq. (19). In the limit of low temperatures the divergence behaves as  $D \sim T^{-0.91}$ , which is not strong enough to compensate for the  $T^2$  term in Eq. (18a) needed to obtain a nonvanishing energy correction.

smaller and vanishes in the limit that  $T \rightarrow 0$ . This also influences the specific heat as can be seen in Fig. 4(b). In the temperature range of the transition from bounded to unbounded motion, the first-order corrected frozen Gaussian calculations agree well with the fully-coupled thawed Gaussian counterpart. For lower temperatures this is no longer so. The divergence is especially noticeable in the low temperature limit for the specific heat where the first-order correction significantly increases the difference between the fully-coupled thawed Gaussian estimate (which is rather accurate as known from numerically exact computations, see Ref. [14]) and the frozen Gaussian based estimate.

Interestingly, although the first-order correction term at very low temperatures is much larger than the zeroth-order frozen Gaussian estimate (see Fig. 3), it does not lead to any change in the estimate of the ground state energy. As may be seen from Fig. 4(a) the increase of the correction to the partition function is not “fast enough”. This is further demonstrated in Fig. 5, where the difference between the first derivatives of the logarithms of the zeroth-order and first-order partition functions,

$$D = \frac{\partial \ln Z_0}{\partial T} - \frac{\partial \ln Z_1}{\partial T} \quad (19)$$

is plotted vs. the temperature. From Fig. 3 one expects this difference to diverge and this is evidently the case. However, the first-order correction term can lead to a correction for the estimate of the ground state energy only if the temperature derivative diverges as  $T^2$ , as can be seen from Eq. (18a). We find, however, that below a critical temperature the difference of the derivatives behaves as  $D \sim T^{-0.91}$ , and this is not sufficient. As a result the first-order correction to the ground state energy vanishes as found in Fig. 4.

Although the first-order correction term does not lead to a corrected estimate for the ground state energy, it does provide information on the quality of the frozen Gaussian approximation. The ratio  $Z_{C1}/Z_0$  (cf. Fig. 3) and the temperature behavior of the correction to the mean energy [cf. Figs. 4 (a) and 5] provide an objective measure for the correctness of the values

as estimated from the frozen Gaussian approximation. Only at a temperature  $T \approx 12$  K and below it, the correction becomes comparable with the zeroth-order estimate, and thus is no longer small. Approximately at the same temperature the energy correction starts to get smaller. Both outcomes indicate that the quality of the approximation is questionable for lower temperatures. However, the dissociation process described in Ref. [14] appears only at higher temperatures, indicating that the frozen Gaussian approximation accurately reflects the quantum transition from a bounded moiety to dissociation into three free particles.

#### 4. Numerical effort for evaluating the first-order correction

The results presented for the mean energy and the specific heat in Sec. 3 showed that the quality of the first-order corrected frozen Gaussian approximation is similar to the fully-coupled thawed Gaussian method in the interesting range of temperatures. It is therefore of interest to compare their computational cost.

The numerically most expensive part is the imaginary time propagation of the dynamical variables. Since the positions  $\mathbf{q}$  in the zeroth-order frozen Gaussian propagator (4) and the correction operator (7) are the only dynamical variables of a frozen Gaussian propagator, the number of equations of motion for the first-order corrected partition function still scales linearly with the particle number. For  $N$  particles one has to solve  $6N + 2$  equations of motion, in which the time integrations of the averaged potential in the exponential of the propagator and the correction operator [c.f. Eq. (4) and Appendix A] are included. By contrast the number of dynamical variables of the fully-coupled thawed Gaussian propagator scales always quadratically with the number of particles due to the symmetric time-dependent Gaussian width matrix. Counting all dynamical variables of the time-evolved Gaussian approximation [3, 11] one obtains  $3N(3N + 3)/2 + 1$  equations of motion. Thus, the imaginary time propagation of the dynamics is cheaper for the first-order frozen Gaussian partition function.

The first-order correction requires, however, also additional numerical effort. The need for propagating pairs of  $\mathbf{q}$  trajectories for the propagator and the correction operator in Eq. (12b) demands a larger number of sampling points for the Monte Carlo integration in the two sets of positions  $\mathbf{q}$ . Additionally, the time integration in Eq. (12b) has to be evaluated. At this point the importance of an analytical evaluation of the  $\mathbf{x}'$  and  $\mathbf{x}$  integrations in Eq. (12b) as described in Appendix A becomes clear. Owing to this simplification one can do without an additional  $6N$ -dimensional Monte Carlo sampling for the operator product [ $\mathbf{x}$  integration in Eq. (12b)] and the trace ( $\mathbf{x}'$  integration). This drastically reduces the numerical costs. Note that a  $3N$ -dimensional trace integration is already required for the zeroth-order approximation of both the frozen and thawed Gaussian partition functions. It can be and is evaluated analytically in all cases. With the analytical evaluation of the  $\mathbf{x}'$  and  $\mathbf{x}$  integrations there remain  $6N$   $\mathbf{q}$  integrations for the first-order corrected frozen Gaussian partition function and  $3N$  for its zeroth-order thawed Gaussian counterpart.

Because of the different numbers of required sampling points there is no general way for estimating the numerical effort. In the case of the argon trimer the additional effort for the first-order correction outweighs the lower number of equations of motion. We used  $6.5 \times 10^7$  sampling points for the frozen Gaussian with first-order correction and  $1.2 \times 10^7$  for the thawed Gaussian to obtain converged results down to low temperatures of about 1 K. On the same architecture (one Tesla C1060 GPU) the frozen Gaussian first-order calculation resulted in approximately twice the time as the zeroth-order thawed Gaussian. Due to the better scaling of the number of dynamical variables (linear instead of quadratic) one may expect that this relation changes in favor of the first-order frozen Gaussian variant with increasing particle number. However, as the results in this article demonstrate, the information the first-order correction provides on the validity of the Gaussian approximations is at least as important as the improvement of the numerical estimate of the physical values.

## 5. Conclusions and outlook

In this article we introduced first-order corrections to a frozen Gaussian approximation [12] of the Boltzmann operator with application to the thermodynamics of atomic clusters. By using a Gaussian fit of the underlying potential it is possible to evaluate many of the necessary integrations of the correction terms analytically such that the first-order correction becomes viable for systems with “many” degrees of freedom. We applied the correction to a study of the thermodynamics of the argon trimer, whose dissociation process has been investigated recently [7, 14].

The highest value of the correction term is to assess the quality of Gaussian approximations used in the study of thermodynamic properties of high-dimensional systems [1–7, 13, 14]. It is known that these Gaussian approximations are exact in the high-temperature limit but are not necessarily correct at low temperatures. The present study shows that the first-order correction indicates a border temperature below which the results of the approximate propagators become questionable and above which they may be considered to be reliable.

The investigation of the argon trimer revealed that the dissociation process [7] discussed earlier with Gaussian approximations in full detail [14] is correctly described by the frozen Gaussian imaginary time propagator. It appears in the temperature range for which the first-order correction is small. Furthermore, the first-order corrected results are comparable with a fully-coupled thawed Gaussian investigation of the system, i.e., the addition of the first-order correction term improves the thermodynamic estimates. The numerical cost of the first-order corrected frozen Gaussian values is, however, higher than that of the thawed Gaussian partition function.

The series expansion of the Boltzmann operator exists also for thawed Gaussian propagators [17] and has been applied to a one-dimensional system [18]. Since the thawed Gaussian propagator approximates the exact mean energy of the argon trimer at low temperatures better than its frozen Gaussian counterpart discussed here, it will be interesting to see whether this can be

confirmed with the correction term and whether the breakdown of the approximation lies at a lower temperature than the frozen Gaussian results.

Since most effects in rare gas clusters such as structural transformations or dissociations appear at low temperatures [1–7, 13] it will be of value to investigate these properties with the series expansion. The correction term should be used to verify the validity of the Gaussian approximations in these cases, in particular, where strong differences are found between the approximate quantum computations and a purely classical theory [6].

## Acknowledgements

This paper is dedicated to Professor Delgado-Barrio, whose paper on Ar clusters was the central impetus for our present investigation. H.C. is grateful for a Minerva fellowship. This work was supported by a grant of the Israel Science Foundation.

## Appendix A. First-order correction term to the partition function for a potential expressed in terms of Gaussians

The correction operator for the frozen Gaussian imaginary time propagator can be written as [12]

$$\begin{aligned} \langle \mathbf{x}' | C(\tau) | \mathbf{x} \rangle &= \langle \mathbf{x}' | \left( -\frac{\partial}{\partial \beta} - H \right) K_0(\tau) | \mathbf{x} \rangle = \det(\mathbf{\Gamma}) \\ &\times \exp\left( -\frac{\hbar^2}{4} \text{Tr}(\mathbf{\Gamma}) \tau \right) \sqrt{\det\left( 2[\mathbf{1} - \exp(-\hbar^2 \mathbf{\Gamma} \tau)]^{-1} \right)} \\ &\times \exp\left( -\frac{1}{4} [\mathbf{x}' - \mathbf{x}]^T \mathbf{\Gamma} [\tanh(\hbar^2 \mathbf{\Gamma} \tau / 2)]^{-1} [\mathbf{x}' - \mathbf{x}] \right) \\ &\times \int \frac{d\mathbf{q}^{3N}}{(2\pi)^{3N}} \Delta V(\mathbf{x}', \mathbf{x}, \mathbf{q}(\tau/2)) \exp\left( -2 \int_0^{\tau/2} d\tau' \langle V(\mathbf{q}(\tau')) \rangle \right. \\ &\quad \left. - [\bar{\mathbf{x}} - \mathbf{q}(\tau/2)]^T \mathbf{\Gamma} [\bar{\mathbf{x}} - \mathbf{q}(\tau/2)] \right), \quad (\text{A.1a}) \end{aligned}$$

where the energy difference operator is found to be

$$\begin{aligned} \Delta V(\mathbf{x}', \mathbf{x}, \mathbf{q}(\tau/2)) &= \frac{\hbar^2}{4} \left( -\text{Tr}(\mathbf{\Gamma}) + [\mathbf{x}' - \mathbf{x}]^T \frac{\mathbf{\Gamma}^2}{2} [\mathbf{x}' - \mathbf{x}] \right) \\ &+ \langle V(\mathbf{q}(\tau/2)) \rangle + \frac{\hbar^2}{2} \left( [\bar{\mathbf{x}} - \mathbf{q}(\tau/2)]^T \mathbf{\Gamma}^2 [\bar{\mathbf{x}} - \mathbf{q}(\tau/2)] \right. \\ &\quad \left. + [\mathbf{x}' - \mathbf{x}]^T \mathbf{\Gamma} \coth\left( \frac{\hbar^2 \tau}{2} \mathbf{\Gamma} \right) \mathbf{\Gamma} [\bar{\mathbf{x}} - \mathbf{q}(\tau/2)] \right) \\ &\quad + [\bar{\mathbf{x}} - \mathbf{q}(\tau/2)] \cdot \langle \nabla V(\mathbf{q}(\tau/2)) \rangle - V(\mathbf{x}'). \quad (\text{A.1b}) \end{aligned}$$

Since most parts of the propagator (4) and of the correction operator (A.1a) include only simple Gaussians or polynomials in  $\mathbf{x}$  and  $\mathbf{x}'$  the matrix element of the product of the zeroth-order propagator and the correction operator needed for computation of the first-order correction term may be calculated analytically. Only the parts including the potential require in general a numerical computation. However, assuming a Gaussian form (14)

for the potential enables one to calculate this part analytically as well. That is, all  $\mathbf{x}'$  and  $\mathbf{x}$  integrations can be performed analytically and only the  $\mathbf{q}$  and  $\tau$  integrations remain for the numerical evaluation. After evaluating the  $\mathbf{x}'$  and  $\mathbf{x}$  integrations in Eq. (12b) we can write the first-order correction as

$$\begin{aligned}
Z_{C1}(\beta) &= \frac{\det(\mathbf{\Gamma})^2}{(2\pi)^N} \exp\left(-\frac{\hbar^2}{4}\text{Tr}(\mathbf{\Gamma})\beta\right) \\
&\times \int_0^\beta d\tau \sqrt{\det([\mathbf{1} - \exp(-\hbar^2\mathbf{\Gamma}(\beta - \tau))]^{-1})} \\
&\times \sqrt{\det([\mathbf{1} - \exp(-\hbar^2\mathbf{\Gamma}\tau)]^{-1})} \\
&\times \int d\mathbf{q}_1^{3N} \int d\mathbf{q}_2^{3N} \Delta V_S(\mathbf{q}_1, \mathbf{q}_2, \beta, \tau) \\
&\times \exp\left(-2 \int_0^{(\beta-\tau)/2} d\tau' \langle V(\mathbf{q}_1(\tau')) \rangle\right) \\
&\times \exp\left(-2 \int_0^{\beta/2} d\tau' \langle V(\mathbf{q}_2(\tau')) \rangle\right), \quad (\text{A.2})
\end{aligned}$$

where the single trajectory contribution to the energy difference operator is denoted as

$$\begin{aligned}
\Delta V_S(\mathbf{q}_1, \mathbf{q}_2, \beta, \tau) &= \exp\left(-\frac{1}{2}\Delta\mathbf{q}(\beta, \tau)^T \mathbf{\Gamma} \Delta\mathbf{q}(\beta, \tau)\right) \\
&\times \left\{ \frac{1}{\sqrt{\det(\mathbf{B}(\beta, \tau)) \det(2\mathbf{\Gamma})}} \left[ \frac{\hbar^2}{4} \left(-\frac{1}{2}\text{Tr}(\mathbf{\Gamma})\right) \right. \right. \\
&+ \frac{1}{4}\text{Tr}(\mathbf{B}(\beta, \tau)^{-1}\mathbf{\Gamma}^2) + \frac{1}{2}\Delta\mathbf{q}(\beta, \tau)^T \mathbf{\Gamma}^2 \Delta\mathbf{q}(\beta, \tau) \\
&+ \langle V(\mathbf{q}_2(\tau/2)) \rangle + \frac{1}{2}\Delta\mathbf{q}(\beta, \tau)^T \langle \nabla V(\mathbf{q}_2(\tau/2)) \rangle \\
&\left. \left. - V_{SG}(\bar{\mathbf{q}}, \beta, \tau) \right\}, \quad (\text{A.3})
\end{aligned}$$

the difference trajectory is defined as

$$\Delta\mathbf{q}(\beta, \tau) = \mathbf{q}_1((\beta - \tau)/2) - \mathbf{q}_2(\tau/2), \quad (\text{A.4a})$$

and the middle point is

$$\bar{\mathbf{q}}(\beta, \tau) = \frac{1}{2}(\mathbf{q}_1((\beta - \tau)/2) + \mathbf{q}_2(\tau/2)). \quad (\text{A.4b})$$

The integrated potential  $V_{SG}(\bar{\mathbf{q}}, \beta, \tau)$  can be written in a form similar to the Gaussian average of the Gaussian fitted potential (14), which was introduced by Frantsuzov et al. [3] for a fully-correlated multi-dimensional Gaussian propagator. It consists of a sum of Gaussians,

$$\begin{aligned}
V_{SG}(\bar{\mathbf{q}}, \beta, \tau) &= \sqrt{\frac{\det(\mathbf{C}(\beta, \tau))}{\det(\mathbf{B}(\beta, \tau) + \mathbf{\Gamma}/2)}} \\
&\times \sum_{j<i} \sum_p c_p \sqrt{\frac{\det(\mathbf{D}_{ij}(\beta, \tau))}{\det(\mathbf{D}_{ij}(\beta, \tau) + \alpha_p)}} \\
&\times \exp\left(-\left[\bar{\mathbf{q}}_i(\beta, \tau) - \bar{\mathbf{q}}_j(\beta, \tau)\right]^T \mathbf{F}_{ij}^{(p)}(\beta, \tau) \left[\bar{\mathbf{q}}_i(\beta, \tau) - \bar{\mathbf{q}}_j(\beta, \tau)\right]\right), \quad (\text{A.5})
\end{aligned}$$

with the matrices

$$\mathbf{B}(\beta, \tau) = \frac{1}{4}\mathbf{\Gamma} \left[ \tanh(\hbar^2\mathbf{\Gamma}(\beta - \tau)/2)^{-1} + \tanh(\hbar^2\mathbf{\Gamma}\tau/2)^{-1} \right] \quad (\text{A.6a})$$

and

$$\mathbf{C}(\beta, \tau) = \frac{1}{2} \left( \mathbf{B}(\beta, \tau) + \frac{\mathbf{\Gamma}}{2} \right) [\mathbf{B}(\beta, \tau)\mathbf{\Gamma}]^{-1}. \quad (\text{A.6b})$$

The submatrices  $\mathbf{C}_{ij}(\beta, \tau)$  for the particles  $i$  and  $j$  of  $\mathbf{C}(\beta, \tau)$  are required for

$$\mathbf{D}_{ij}(\beta, \tau) = \left( \mathbf{C}_{ii}(\beta, \tau) + \mathbf{C}_{jj}(\beta, \tau) - \mathbf{C}_{ij}(\beta, \tau) - \mathbf{C}_{ji}(\beta, \tau) \right)^{-1} \quad (\text{A.7a})$$

and

$$\mathbf{F}_{i,j}^{(p)}(\beta, \tau) = \alpha_p - \alpha_p^2 \left( \alpha_p + \mathbf{D}_{ij}(\beta, \tau) \right)^{-1}. \quad (\text{A.7b})$$

In Eq. (A.3) one can clearly see that due to the Gaussian in  $\Delta\mathbf{q}$  the contribution of a pair of trajectories  $\mathbf{q}_1(\tau)$  and  $\mathbf{q}_2(\tau)$  will only be nonvanishing if the distance between them is small. This implies that the restriction of  $\mathbf{q}_1$  to the confining sphere defined by  $R_c$  will automatically impose a restriction on  $\mathbf{q}_2$ .

## References

- [1] J. P. Neirotti, D. L. Freeman, J. D. Doll, A heat capacity estimator for Fourier path integral simulations, *J. Chem. Phys.* 112 (2000) 3990–3996.
- [2] C. Predescu, D. Sabo, J. D. Doll, D. L. Freeman, Heat capacity estimators for random series path-integral methods by finite-difference schemes, *J. Chem. Phys.* 119 (2003) 12119–12128.
- [3] P. A. Frantsuzov, V. A. Mandelshtam, Quantum statistical mechanics with Gaussians: Equilibrium properties of van der Waals clusters, *J. Chem. Phys.* 121 (2004) 9247–9256.
- [4] C. Predescu, P. A. Frantsuzov, V. A. Mandelshtam, Thermodynamics and equilibrium structure of  $\text{Ne}_{38}$  cluster: Quantum mechanics versus classical, *J. Chem. Phys.* 122 (2005) 154305.
- [5] R. P. White, S. M. Cleary, H. R. Mayne, Phase changes in Lennard-Jones mixed clusters with composition  $\text{Ar}_n\text{Xe}_{6-n}$  ( $n = 0, 1, 2$ ), *J. Chem. Phys.* 123 (2005) 094505.
- [6] P. A. Frantsuzov, D. Meluzzi, V. A. Mandelshtam, Structural transformations and melting in neon clusters: Quantum versus classical mechanics, *Phys. Rev. Lett.* 96 (2006) 113401.
- [7] R. Pérez de Tudela, M. Márquez-Mijares, T. González-Lezana, O. Roncero, S. Miret-Artés, G. Delgado-Barrio, P. Villarreal, A path-integral Monte Carlo study of a small cluster: The Ar trimer, *J. Chem. Phys.* 132 (2010) 244303.
- [8] B. J. Berne, D. Thirumalai, On the simulation of quantum systems: Path integral methods, *Annu. Rev. Phys. Chem.* 37 (1986) 401–424.
- [9] N. Makri, Time-dependent quantum methods for large systems, *Annu. Rev. Phys. Chem.* 50 (1999) 167–191.
- [10] D. M. Ceperley, Metropolis methods for quantum Monte Carlo simulations, *AIP Conf. Proc.* 690 (2003) 85–98.
- [11] P. Frantsuzov, A. Neumaier, V. A. Mandelshtam, Gaussian resolutions for equilibrium density matrices, *Chem. Phys. Lett.* 381 (2003) 117–122.
- [12] D. H. Zhang, J. Shao, E. Pollak, Frozen Gaussian series representation of the imaginary time propagator theory and numerical tests, *J. Chem. Phys.* 131 (2009) 044116.
- [13] P. A. Frantsuzov, V. A. Mandelshtam, Equilibrium properties of quantum water clusters by the variational Gaussian wavepacket method, *J. Chem. Phys.* 128 (2008) 094304.

- [14] H. Cartarius, E. Pollak, Imaginary time Gaussian dynamics of the Ar<sub>3</sub> cluster, *J. Chem. Phys.* 134 (2011) 044107.
- [15] J. Liu, W. H. Miller, Using the thermal Gaussian approximation for the Boltzmann operator in semiclassical initial value time correlation functions, *J. Chem. Phys.* 125 (2006) 224104.
- [16] D. D. Frantz, D. L. Freeman, J. D. Doll, Extending J walking to quantum systems: Applications to atomic clusters, *J. Chem. Phys.* 97 (1992) 5713–5731.
- [17] J. Shao, E. Pollak, A new time evolving Gaussian series representation of the imaginary time propagator, *J. Chem. Phys.* 125 (2006) 133502.
- [18] R. Conte, E. Pollak, Comparison between different Gaussian series representations of the imaginary time propagator, *Phys. Rev. E* 81 (2010) 036704.
- [19] S. Zhang, E. Pollak, Monte Carlo method for evaluating the quantum real time propagator, *Phys. Rev. Lett.* 91 (2003) 190201.
- [20] E. Pollak, J. Shao, Systematic improvement of initial value representations of the semiclassical propagator, *J. Phys. Chem. A* 107 (2003) 7112–7117.
- [21] T. González-Lezana, J. Rubayo-Soneira, S. Miret-Artés, F. A. Gianturco, G. Delgado-Barrio, P. Villarreal, Comparative configurational study for He, Ne, and Ar trimers, *J. Chem. Phys.* 110 (1999) 9000–9010.
- [22] R. D. Etters, J. Kaelberer, Thermodynamic properties of small aggregates of rare-gas atoms, *Phys. Rev. A* 11 (1975) 1068–1079.